ENHANCED TENSILE DUCTILITY OF METALLIC GLASS MATRIX COMPOSITES WITH NOVEL MICROSTRUCTURE

Yunpeng Jiang

State Key Laboratory of Mechanics and Control of Mechanical, Nanjing University of Aeronautics and Astronautics, Nanjing 210016, China
ypjiang@nuaa.edu.cn

Keywords: Metallic glass, Microstructure, Finite element method (FEM)

ABSTRACT

In this contribution, numerical study was conducted to reveal the effects of particle concentration and particle morphology on the tensile behaviors of metallic glass (MG) matrix composites. Free volume acts as an internal state variable to depict the nucleation, growth and coalescence of shear bands in the MG matrix composites on the basis of free volume theory, which was incorporated into the ABAQUS code as a user material subroutine UMAT. The impedance efficiency of various microstructures on the propagation of shear bands was discussed, and whereby a novel network configuration of second-phase was suggested to improve MG's tensile plasticity. The present work is helpful to understand the failure mechanisms and the tensile toughening design of MG matrix composites.

1 INTRODUCTION

In order to overcome the intrinsic brittleness of metallic glasses (MGs), introducing second-phase in the MG matrix to make the heterogeneous composites is the most effective measure [1]. Up to date, some inorganic powders, such as SiC, SiO_2, Mg, Mo and graphite powders, were dispersed in the Mg-, Zr-, and Ti based MGs to make *ex-situ* composites [2-3]; and many kinds of *in-situ* composites were directly synthesized [4-5].

Many innovative works have been performed to explore the potential feasibility of improving the tensile plasticity of MGs. Sopu et al. [6] numerically studied pore density, distribution, size and number on the deformation behavior of nanoporous $Cu_{64}Zr_{36}$ glass by using both molecular dynamics and FEM. Sarac et al. [7] discussed the influence of the pores on the mechanical properties of MGs, and found that the pore configuration, overall porosity and diameter to the spacing ratio of the pores affect the resulting plastic deformation. Shete et al. [8-9] performed finite strain continuum FEM to reflect the role played by the volume fraction and strain hardening behavior of crystalline particles on the strength and ductility of the composites. Wang et al. [10] numerically analyzed the effect of initial free volume gradient distribution on the mechanical behaviors of MGs, and pointed out that the gradient degree greatly affects both the strength and ductility.

In this work, free volume theory is adopted to characterize the shear band evolution in the MG matrix, and then effect of particle concentration and morphology on the tensile behaviors of MG matrix composites is studied. With increasing particle concentration, particles will form an interconnecting network morphology, and effectively restrict the free propagation of shear bands in the MG matrix. Motivated by the shear banding mechanism in highly compacted particles filled MG matrix composite, a composite with a novel network microstructure is advanced, and the corresponding toughening mechanisms in such novel composites is revealed. The toughening efficiency by this morphology is compared with discrete particles filled composites.

2 CONSTITUTIVE RELATIONS OF MG

The shear-band initiation, growth, and propagation form the fundamental deformation mechanism in MGs. At the microscopic scale, shear-band formation is believed to be associated with the evolution of the local structural order. One atomistic mechanism capturing shear-band formation and evolution in MGs is the free volume theory developed by Spaepen [11] and further extended by Steif [12]. From a

continuum mechanics point of view, the shear-band is a result of strain softening and considered to be a strain localization phenomenon. The free volume model regards free volume as an internal state variable, which controls the structural evolution at the atomic level in MGs.

According to the J_2-type, small strain visco-plasticity framework, the free volume theory is extended to a multi-axial stress state. The strain rate is decomposed into the elastic and plastic parts

$$\dot{\varepsilon}_{ij} = \dot{\varepsilon}^{e}_{ij} + \dot{\varepsilon}^{p}_{ij} \tag{1}$$

The above elastic part is expressed by the general Hooke's law:

$$\dot{\varepsilon}^{e}_{ij} = \frac{1+\nu}{E}\left(\dot{\sigma}_{ij} - \frac{\nu}{1+\nu}\dot{\sigma}_{kk}\delta_{ij}\right) \tag{2}$$

with a characteristic time scale $t^*=tf^{-1}\exp(\Delta G^m/k_BT)$, where f denotes the frequency of atomic vibration, E is elastic modulus, ν is Poisson's ratio, ΔG^m is the activation energy, k_B is the Boltzmann constant, and T is the absolute temperature. Based on the normalized time t^*, the equations are differentiated in terms of the normalized time scale t^*. The plastic part is rewritten as [13]:

$$\dot{\varepsilon}^{p}_{ij} = \exp\left(-\frac{1}{\nu_f}\right)\sinh\left(\frac{\sigma_e}{\sigma_0}\right)\frac{S_{ij}}{\sigma_e} \tag{3}$$

where v_f denotes the average free volume per atom, $\sigma_0=2k_BT/\Omega$ is the reference stress, $S_{ij}=\sigma_{ij} - \sigma_{kk}\delta_{ij}/3$ is the deviatoric stress tensor, and $\sigma_e=(S_{ij}S_{ij})^{1/2}$ is the von Mises' stress. It should be noting that a dot over a quantity X denotes $(\dot{X})= f^{-1}\exp(\Delta G^m/k_BT)(\partial X/\partial t)$, which is used in the following expression. The free volume evolution equation in the multi-axial stress state is expressed as:

$$\dot{v}_f = \frac{1}{\alpha}\exp\left(-\frac{1}{\nu_f}\right)\left\{\frac{3(1-\nu)}{E}\left(\frac{\sigma_0}{\beta\nu_f}\right)\left(\cosh\left(\frac{\sigma_e}{\sigma_0}\right)-1\right)-\frac{1}{n_D}\right\} \tag{4}$$

where α stands for a geometric factor of order 1; $\sigma_0=2k_BT/\Omega$ is the reference stress, v_f is the average free volume per atom, $v_f=v_f/\alpha v^*$ is the normalized free volume, $\beta=v^*/\Omega$, and n_D is the number of atomic jumps needed to annihilate a free volume equal to v^*, and is usually taken to be 3~10.

3 FEM SIMULATION

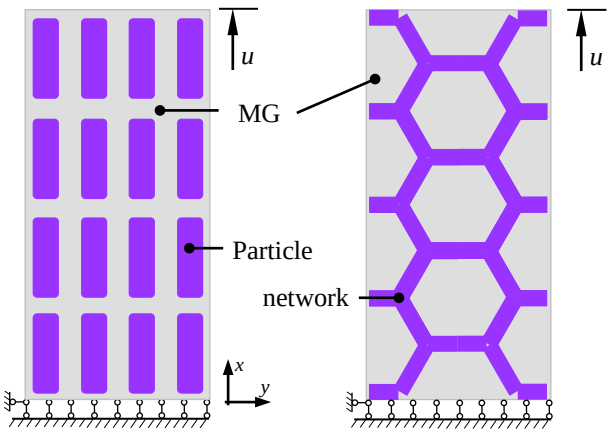

(*a*) particle composite (*b*) network composite

Fig. 1 Computational model adopted in ABAQUS package for 2D modeling of plane-strain tension and the corresponding boundary conditions exerted during the computation for particle filled composite (a) and for network composites (b).

In this simulation, the shear band evolution is described by an *internal state variable*, i.e. the normalized free volume v_f as given in Eq. (3). The initially undeformed numerical model of this sample as shown in **Fig. 1** for particle filled composites in (a) and network composites (b). During the computation, all the nodes in the bottom node set are prevented from motion along axis-*x*. A positive displacement along axis-*x* is exerted to the single node located at the top-right corner with the desired test strain-rate. The multi-point constraint (MPC) equation is applied to the rest of the nodes along the top surface in order to keep their deformation coordinate with the top-right corner node.

In order to better reflect the shear localization in the MGs, some elements with a slightly lower value of initial free volume act as nucleation sites for shear banding. The initial free volume v_0 was presumed to be statistically varied over the elements obeying a Gaussian distribution function with a mean value of 0.05, and a standard deviation of 0.005. The ductile particles should obey the following yielding principle,

$$\frac{\varepsilon_{eq}}{\varepsilon_y}=\left(\frac{\sigma_{eq}}{\sigma_y}\right)^{\frac{1}{N}}-1,\ \sigma_{eq}\geq\sigma_y \tag{5}$$

where σ_y, σ_{eq}, ε_y and ε_{eq} are the yielding stress, von Mises's stress, yielding strain and equivalent strain, respectively. N is the strain hardening coefficient, and will be discussed by changing its value. The material properties for the MG matrix are: E=100GPa, v=0.38, n_D=3, α=0.21, β=1.0 and σ_0=94MPa. Those properties for the particle phase are: E=150GPa, v=0.35, ε_y=0.0067 and σ_y=1.2GPa.

4 RESULTS AND DISCUSSION

4.1 *Effect of particle number density*

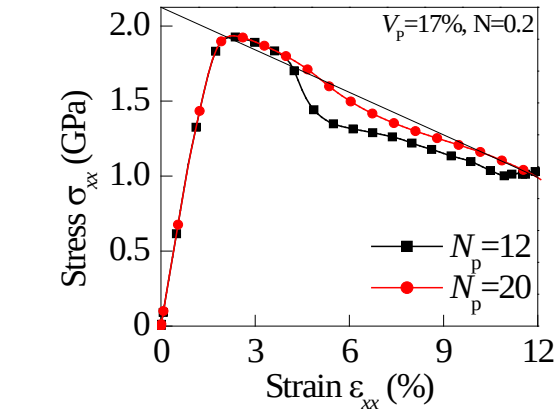

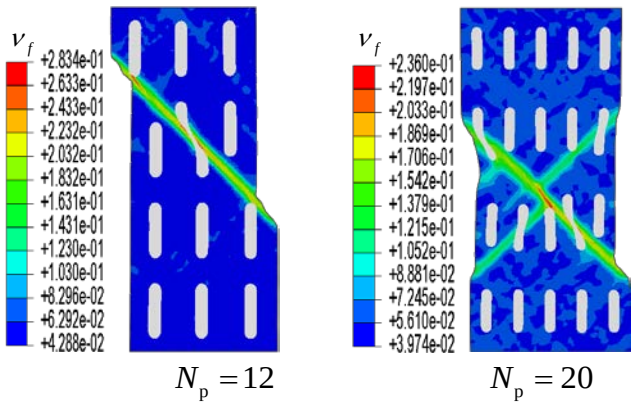

$N_p=12$ $N_p=20$

Fig. 2 Dependence of the stress–strain relations on the particle spacing and the corresponding snapshots of shear banding formation at the tensile strain ε_{xx}=10%.

Fig. 2 presents the dependence of the stress–strain relations on the particle spacing and the resulting snapshots of shear band formation at the tensile strain ε_{xx}=10%. At a given particle concentration V_p=17%, the composites with 12 and 20 particles shows different tensile plasticity, and MG matrix composite with more particles is much better in the plasticity. Only a main shear band happens in the composites with 12 particles, while multiple shear bands appear in the composite with 20 particles. The resulting big difference is mainly caused by the two following reasons: (1) After introducing many more particles, the local stress field should be more complicated, and consequently the probability to initiate a shear band also increases, which contributes to the formation of multiple shear bands and their intersection; (2) The spacing between particles decreases with increasing particle numbers or decreasing particle size, which indicates that many more particles may locate in the propagation path of shear banding.

4.2 *Effect of network morphology*

Fig. 3 gives the comparison between the stress-strain relations of particle filled and network composites. The present modeling clearly confirmed the feasibility of adopting a novel network microstructure in improving the tensile ductility of MGs. The network morphology successfully divides the MG matrix into many isolated segments as shown in the associated contours, in which the mature shear bands are not easily to happen, and thus the collapse damage is avoided. As for the network second phase, the influence of interface separation would not be very important, since the network second phase should across over the whole sample, and thus the two phases share the applied loading through the whole deformation.

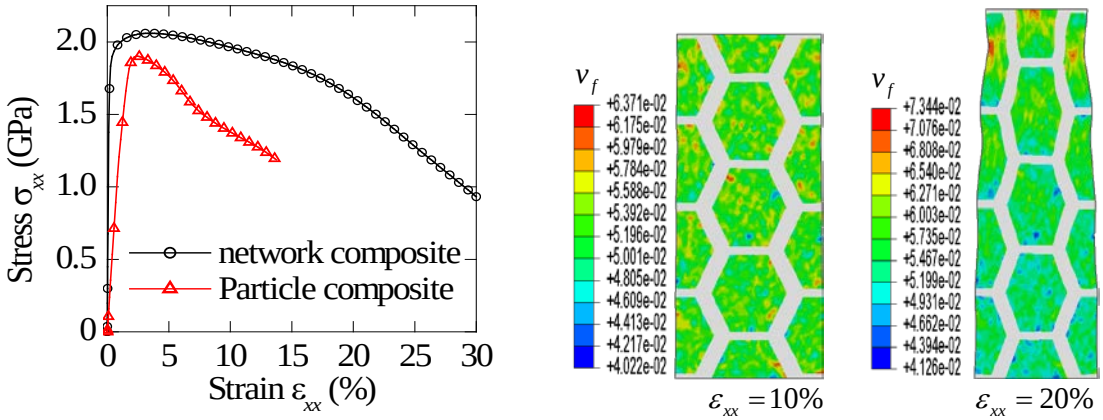

Fig. 3 Comparison between the stress-strain relations of particle filled and network composites (V_p=30%, and N=0.2), and the shear band evolution in network composite is associated.

Moreover, the reliance of the mechanical performance of such composites on 'particle' volume fraction and strain hardening coefficient was fatherly analyzed as shown in **Fig. 4**. The similar conclusions could be reached, the increase in the 'particle' volume fraction and the strain hardening coefficient can improve the tensile plasticity of MG matrix composites.

5 CONCLUSION

Free volume theory-based FEM was referred to analyze the effect of particle concentration and particle morphology on the tensile behaviors of MG matrix composites. Discussing the shear banding in various microstructures could establish the dependence of tensile plasticity of MG matrix composites on the particle volume fraction and morphology. Several main conclusions are reached,

(1). Increasing particle number density can effectively improve the tensile plasticity of MG matrix composites;
(2). As compared to discrete particle filled composites, the network morphology of second-phase should be more efficient in improving the tensile plasticity of MG matrix composites.

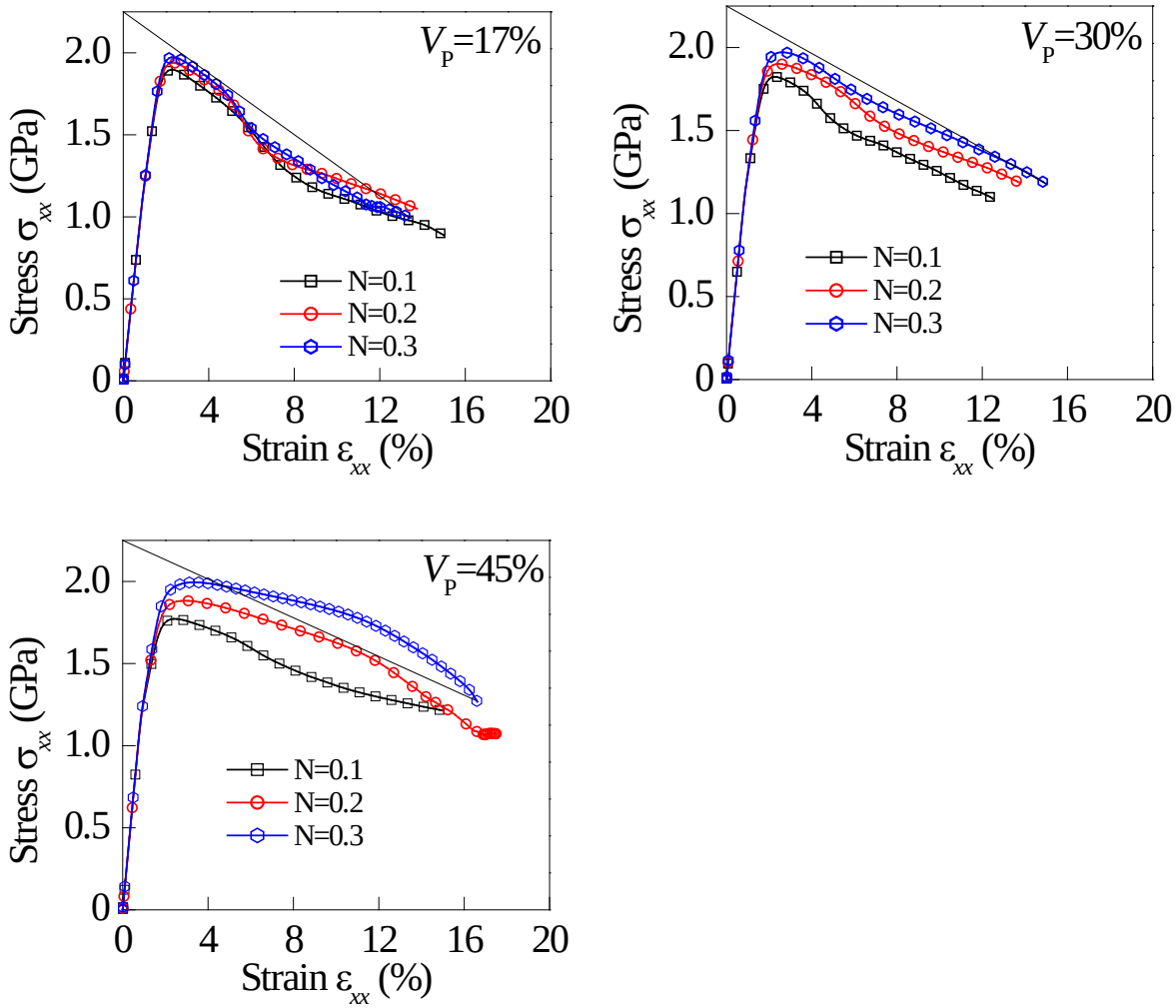

Fig. 4 Dependence of the stress–strain relations on the second-phase concentration and strain hardening coefficients for network composites.

Acknowledgement

This work was supported by the Fundamental Research Funds for the Central Universities (YAH16056), Jiangsu Provincial Natural Science Foundation (BK2012407) and Program for New Century Excellent Talents in University (NCET-12-0840)

REFERENCES

[1] J.W. Qiao, H.L. Jia and P.K. Liaw. *Mater Sci Eng R* **100**(2016): 1–69.
[2] J.S.C. Jang, T.H. Li, S.R. Jian, J.C. Huang and T.G. Nieh. *Intermetallics* **19**(2011): 738–743.
[3] M.E. Siegrist and J.F. Loffler. *Scripta Mater* **56**(2007): 1079–1082.

[4] R.L. Narayan, P.S. Singh, D.C. Hofmann, N. Hutchinson, K.M. Flores and U. Ramamurty. Acta *Mater* **60**(2012): 5089–5100.
[5] D.C. Hofmann, J.Y. Suh, A. Wiest, G. Duan, M.L. Lind, M.D. Demetriou and W.L. Johnson. *Nature* **451**(2008): 1085–1089.
[6] D. Sopu, C. Soyarslan, B. Sarac, S. Bargmann, M. Stoica and J. Eckert. *Acta Mater* 106(2016): 199–207.
[7] B. Sarac, B. Klusemann, T. Xiao and S. Bargmann. *Acta Mater* 77(2014): 411–422.
[8] M.K. Shete, T. Dutta, I. Singh, R. Narasimhan and U. Ramamurty. Intermetallics 83(2017): 70–82.
[9] M.K. Shete, I. Singh, R. Narasimhan and U. Ramamurty. *Scrip Mater* 124(2016): 51–55.
[10] Y.W. Wang, M. Li and J.W. Xu. *Script Mater* 130(2017): 12–16.
[11] F. Spaepen. *Acta Metall* **25**(1977): 407–415.
[12] P.S. Steif, F. Spaepen and J.W. Hutchinson. *Acta Metall* **30**(1982): 447–455.
[13] Y.F. Gao. Modell *Simul Mater Sci Eng* **14**(2006): 1329–1345.